$Ni(CO)_4$ and $Fe(CO)_5$. A Study of Molecular Recognition and Crystal Construction

Dario Braga,* Fabrizia Grepioni,* and A. Guy Orpen*

Dipartimento di Chimica G. Ciamician, Università di Bologna, Via Selmi 2, 40126 Bologna, Italy, and School of Chemistry, University of Bristol, Bristol BS8 1TS, U.K.

Received June 2, 1994®

The molecular organization in crystals of the prototypical organometallic molecules $Ni(CO)_4$ and $Fe(CO)_5$ has been investigated by means of packing potential energy calculations and computer graphic analysis. The atom–atom pairwise potential energy method has been used to study the interaction energy between molecular pairs and the molecular self-recognition process that leads to crystal construction. Alternative crystal structures have been generated for the two molecules and for the hypothetical square-pyramidal isomer of $Fe(CO)_5$.

Introduction

The idea of predicting the crystal structure of a given molecular compound is both fascinating to structural chemists and crystallographers and important to materials scientists and others intent on applications of solids. Until recently, attention has been mainly focused on the molecular geometry and the interatomic structural parameters of the individual molecular entity. Considerable progress has been made in the understanding of the chemical bonding and of the relationship between structure and chemical reactivity. The theory of interatomic bonding is so well established that even complex molecular species, such as organometallic compounds, can be understood and interpreted also with the help of ab-initio or semiempirical methods.[1] This is not so for the intermolecular interactions that are responsible for the formation and stability of molecular aggregates in solids. There is an increasing awareness of the importance of intermolecular interactions, since they determine the organization of molecules or ions in the crystal and therefore the physico-chemical properties of the crystalline material.[2] That is to say that the molecular self-recognition process, which is the basis of the crystallization process, leads to a *new chemical system* with its own characteristics, a very complex supramolecule whose properties will depend on *the physical and chemical properties of the component molecule or ion, as well as on those resulting from the intermolecular interactions in the crystal structure.*

We have initially attempted to interpret the observed crystal packings of neutral and ionic organometallic complexes and clusters in order to gain information on the relationship between size, shape, and charge of the component particles and on the molecular organization in the solid state.[3] To this end, we have developed methods based on atom–atom packing potential energy calculations[4] and computer graphics that allow us to scan the immediate surroundings of one reference molecule or ion[5] and to identify the closest neighbors in the first coordination sphere (or enclosure shell).[6] This approach allows a direct study of the packing motifs and of the factors responsible for crystal cohesion and stability and has been useful in some cases in the study of the relationship between *molecular and crystal structures*. The problems tackled in this way range from organometallic polymorphism[7a] to the packing of small and large nuclearity cluster molecules[7b] to the cation control on the packing organization in the lattice of organometallic molecular salts.[7c,d]

In the following we report some results of our attempts to *generate* crystal structure starting from molecular structure alone. For reasons given below we have chosen $Ni(CO)_4$ and $Fe(CO)_5$ as our benchmark molecules. Clearly, the following procedures can be applied whenever the molecular structure is available, whether derived from an ab-initio study or experimentally established by means of any other structural technique in solution or in the gas phase.

The possibility of generating hypothetical crystal structures from known molecular structures has always been attractive for structural chemists.[8a] All previous work in this direction has been carried out in the field of solid state organic chemistry with remarkable achievements. The study of the packing modes of aromatic hydrocarbons,[8b] as well as the investigation of the crystal structure organization of adipamide[8c,d] are two

® Abstract published in *Advance ACS Abstracts*, July 15, 1994.

(1) See, for example: (a) Albright, T. A.; Burdett, J. K.; Whangboo, M.-H. *Orbital Interactions in Chemistry*; John Wiley & Sons, Interscience Publishers: New York, 1985. (b) Allinger, N. L.; Yuh, Y. H.; Lii, J.-H. *J. Am. Chem. Soc.* **1989**, *111*, 8551.

(2) See, for example: *Structure and Properties of Molecular Crystals*; Pierrot, M., Ed.; Elsevier: Dordrecht, The Netherlands, 1990; p 235. Desiraju, G. R. *Crystal Engineering, The Design of Organic Solids*; Elsevier: Amsterdam, 1989; p 47. Braga, D. *Chem. Rev.* **1992**, *92*, 633. Rouxel, J. *Acc. Chem. Res.* **1992**, *25*, 328. Braga, D.; Grepioni, F. *Acc. Chem. Res.* **1994**, *27*, 51.

(3) (a) Braga, D.; Grepioni, F. *Organometallics* **1991**, *10*, 1254. (b) Braga, D.; Grepioni, F.; Johnson, B. F. G.; Lewis, J.; Housecroft, C. E.; Martinelli, M. *Organometallics* **1991**, *10*, 1260. (c) Braga, D.; Grepioni, F.; Johnson, B. F. G.; Dyson, P.; Frediani, P.; Bianchi, M.; Piacenti, F.; Lewis, J. *J. Chem. Soc., Dalton Trans.* **1992**, 2565. (d) Braga D.; Grepioni, F. *Organometallics* **1991**, *10*, 2563. (e) Braga, D.; Grepioni, F. *Organometallics* **1992**, *11*, 711.

(4) (a) Kitaigorodsky, A. I. *Molecular Crystal and Molecules*; Academic Press: New York, 1973. (b) Pertsin, A. J.; Kitaigorodsky, A. I. *The Atom-Atom Potential Method*; Springer-Verlag: Berlin, 1987. (c) Gavezzotti, A.; Simonetta, M.; *Chem. Rev.* **1982**, *82*, 1.

(5) Braga, D.; Grepioni, F.; Righi, S.; Johnson, B. F. G.; Frediani, P.; Bianchi, M.; Piacenti, F.; Lewis, J. *Organometallics* **1991**, *10*, 706. Braga, D.; Grepioni, F. *J. Chem. Soc., Dalton Trans.* **1993**, 1223.

(6) Braga, D.; Grepioni, F.; Sabatino, P. *J. Chem. Soc., Dalton Trans.* **1990**, 3137.

(7) (a) Braga, D.; Grepioni, F.; Dyson, P. J.; Johnson, B. F. G.; Frediani, P.; Bianchi, M.; Piacenti *J. Chem. Soc., Dalton Trans.* **1992**, 2565. (b) Braga, D.; Grepioni, F. *Organometallics* **1992**, *10*, 1254. (c) Braga, D.; Grepioni, F. *Organometallics* **1992**, *11*, 1256. (d) Braga, D.; Grepioni, F.; Milne, P.; Parisini, E. *J. Am. Chem. Soc.* **1993**, *115*, 5115.

0276-7333/94/2313-3544$04.50/0

examples worth mentioning. More recently, this type of approach has been further developed by Gavezzotti to generate crystal structures for low-polarity organic compounds.[9]

We have chosen to study $Ni(CO)_4$ and $Fe(CO)_5$ because they possess prototypical molecular shapes, viz. the tetrahedron and the trigonal bipyramid, respectively.[10] The two kinds of CO-ligand arrangements are different (OC—Ni—CO 109.5°; OC—Fe—CO equatorial–equatorial 120°; OC—Fe—CO axial–equatorial 90°), thus constituting a basic and representative sample for our molecular recognition and crystal construction study. The two molecules are, on the other hand, *sufficiently similar* that the potential parameters for the intermolecular interactions in the observed (and calculated) crystals of the two species can be assumed to be the same.

Another reason of interest arises from the different degree of structural flexibility of the two molecules. On the basis of CSA (chemical shift anisotropy) analysis and spin–lattice relaxation time measurements it has been shown that $Ni(CO)_4$ is static on the NMR time scale at room temperature, while CO exchange via Berry pseudorotation (i.e. via an intermediate complementary square-pyramidal geometry) is apparently taking place in solid $Fe(CO)_5$ at room temperature.[11] A more recent variable temperature CPMAS study reveals below 235 K two resonances with an integrated intensity ratio of 2:3, while between 243 and 250 K three resonances are observed.[12] This behavior has been interpreted as a rotational motion around the 3-fold axis rather than by an axial–equatorial exchange process at these lower temperatures.

One basic assumption behind the packing search and crystal construction procedures is that the *molecular* structure is not affected by the different packing arrangements. This is an acceptable approximation in the case of $Ni(CO)_4$ (that is known to be rigid in the solid state), while caution should be exercised in the case of fluxional $Fe(CO)_5$. As a matter of fact we will take advantage of this flexibility in our attempt to generate hypothetical crystal structures for the intermediate of the Berry pseudorotation interconversion pathway, namely a square-pyramidal isomer of $Fe(CO)_5$ (see below).

Description of the Observed Crystal Structures of $Ni(CO)_4$ and $Fe(CO)_5$

$Ni(CO)_4$ and $Fe(CO)_5$ are prototypical compounds, and their *molecular structure* in the solid state has been recently reinvestigated using diffraction data collected for both compounds at two temperatures.[13] We are here interested mainly in the *crystal structure*; details of the *molecular structure* including a thorough analysis of the molecular dynamics in the solid state will be reported in a forthcoming paper.

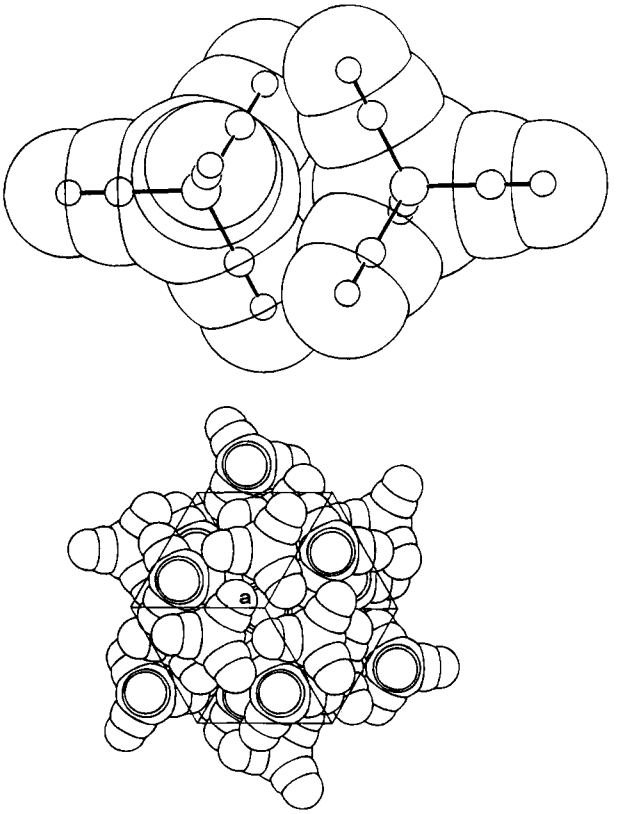

Figure 1. (a, top) "Dimer" formed by two $Ni(CO)_4$ molecules interlocked along the 3-fold axis. The two Ni atoms are at 4.61 Å at 238 K and 4.57 Å at 198 K. (b, bottom) Projection of the packing. The dimeric unit packs in a 3:6:3 cuboctahedral arrangement.

$Ni(CO)_4$ crystallizes in space group $Pa\bar{3}$ with $Z = 8$. As previously noted,[6] in this crystal the dominant interaction is between a pair of molecules related by a center of symmetry. The "dimer" (which has D_{3d} symmetry; see Figure 1a) consists of two $Ni(CO)_4$ molecules interlocked along one of the 3-fold axes with two Ni atoms in close contact (the Ni···Ni separation is 4.61 Å at 238 K and 4.57 Å at 198 K). This is one of the few cases in which a direct metal—metal "van der Waals" contact is observed since in organometallic crystals the metal atoms are usually completely buried inside the ligand shell. The dimeric unit packs in a 3:6:3 cuboctahedral arrangement (Figure 1b). The interlocking along the 3-fold axis is presumably responsible for a minute deviation from *Td* molecular symmetry: the C—Ni—C angle for the three CO's involved in the interlocking is larger than those involving the CO ligand along the 3-fold axis [109.65(6) vs 109.29(6)°].[13]

$Fe(CO)_5$ crystallizes in space group $C2/c$ ($Z = 4$), the crystallographic 2-fold axis going through the Fe atom and one equatorial CO ligand. The preferential interlocking packing motif in this structure is shown in Figure 2a: two neighboring molecules are placed with the *c*-axis parallel to the 3-fold axis of the molecule so

(8) (a) Dauber, P.; Hagler, A. T. *Acc. Chem. Res.* **1980**, *13*, 105. (b) Bernstein, J.; Sarma, J. A. R. P.; Gavezzotti, A. *Chem. Phys. Lett.* **1990**, *174*, 361. (c) Hagler, A. T.; Leiserowitz, L. *J. Am. Chem. Soc.* **1978**, *78*, 5879. (d) Leiserowitz, L.; Hagler, A. T. *Proc. R. Soc. London, A* **1983**, *388*, 133.

(9) Gavezzotti, A. *J. Am. Chem. Soc.* **1991**, *113*, 4622.

(10) (a) Ladell, J.; Post, B.; Fankuchen, I. *Acta Crystallogr.* **1952**, *5*, 795. (b) Hanson, A. W. *Acta Crystallogr.* **1962**, *15*, 930. (c) Donohue, J.; Caron, A. *Acta Crystallogr.* **1964**, *17*, 663. (d) Boese, R.; Bläser, D. *Z. Krystallogr.* **1990**, *193*, 289.

(11) (a) Spiess, H. W.; Grosescu, R.; Haeberlen, U. *Chem. Phys.* **1974**, *6*, 226. (b) Gleeson, J. W.; Vaughan, R. W. *J. Chem. Phys.* **1983**, *78*, 5384.

(12) (a) Hanson, B. E. In *Metal-Metal Bonds and Clusters in Chemistry and Catalysis*; Fackler, J. P., Ed.; Plenum: New York, 1989; p 231. (b) Hanson, B. E. *J. Am. Chem. Soc.* **1989**, *111*, 6442.

(13) Braga, D.; Grepioni, F.; Orpen, A. G. *Organometallics* **1993**, *12*, 1993.

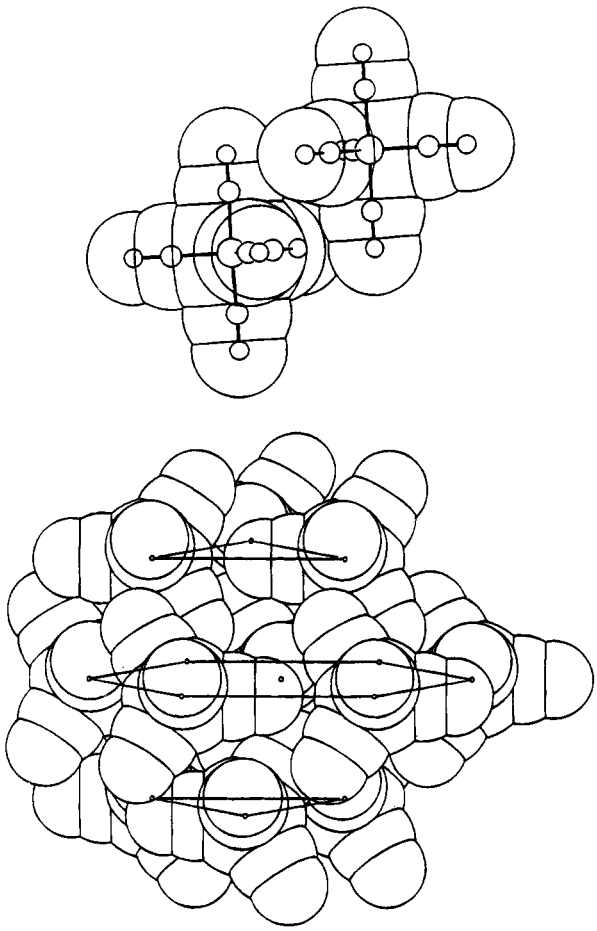

Figure 2. (a, top) Preferential interlocking packing motif in the crystal structure of $Fe(CO)_5$. Two neighboring molecules are parallel to the long axis of the trigonal bipyramid. (b, bottom) Each molecule surrounded by 12 next neighbors, thus resulting in a cuboctahedral packing arrangement, as shown by the thin lines joining the molecular centers.

that the axial CO of one molecule is surrounded by two equatorial ligands of a neighboring molecule. The effect on the molecular geometry is more substantial than for $Ni(CO)_4$: the C—Fe—C angle between the two equatorial CO's embracing the neighboring axial ligand is 121.11(5)° vs 117.78(10)° for the ligands involved in the interaction between molecules piled along the 2-fold axis. The Fe···Fe separation is 5.16 Å. By symmetry each molecule is involved in two such interactions. The resulting packing organization is cuboctahedral (Figure 2b), each molecule being surrounded by 12 next neighbors, as observed in $Mn_2(CO)_{10}$, while $Fe_2(CO)_9$, $Co_2(CO)_8$, and $Cr(CO)_6$ crystallize in *anti*-cuboctahedral fashion.[6]

Computational Procedure

(a) Choice of Potential Parameters. In a previous study[14] we discussed the effects of using two different sets of atom—atom potential energy parameters A, B, and C for the equation $PPE = \sum_i\sum_j[A \exp(-Br_{ij}) - Cr_{ij}^{-6} + q_iq_jr_{ij}^{-1}]$, where r_{ij} represents the nonbonded atom—atom interatomic separation and q the atomic charge. Index i in the summation runs over all atoms of the reference molecule, and index j over all atoms of the surrounding molecules (see refs 3d,e and 6 for more details of the application of the method to organometallic molecules). The parameters A, B, and C were taken from Mirsky[15] (neglecting the Coulombic term q_iq_j/r_{ij}, set named MRK) or from Williams (including the Coulombic term, set named CCW).[16] In the present study, a new set of potential parameters obtained by Gavezzotti and Filippini has been used (set GVF)[17] and compared with MRK. The reason for this choice is 2-fold: first the set CCW requires a rather arbitrary evaluation of atomic or site charges for the Coulombic term in the expression of the atom—atom function; second we were interested in putting the set GVF to test because its statistical basis would make the potentials more transferable and therefore more suitable for the treatment of organometallic systems. The reader is pointed to refs 14—17, for a more detailed discussion of the parameter choice and of the limitations inherent to the application of the atom—atom potential energy method to organometallic crystals. A slightly modified version of the computer program OPEC was used for all calculations of packing potential energies and to estimate packing coefficients and intermolecular interactions.[18] Packing coefficients are calculated from the ratio ZV_{mol}/V_{cell} where V_{mol} is the van der Waals volume of the molecule calculated by Kitaigorodsky's "intersecting cups" method.

(b) Refinement of the Observed Structures. The GVF and MRK parameter sets were tested on the experimentally observed structures of $Ni(CO)_4$ and $Fe(CO)_5$. The tests were run using PCK83[19] that allows an optimization of the packing energies with respect to cell parameters and molecular rigid-body translation and rotation (structure "relaxation" or "refinement"). The results are summarized in Table 1. The working hypothesis is that the best choice of potential parameters (to be subsequently used for crystal construction) is the one producing the smallest displacements from the observed structures.

The following general conditions were applied for the tests: (i) in both cases crystal structure refinement was performed starting from the data collected at the higher temperatures (228 and 238 K, respectively); (ii) the parameters used for the metal atoms were those for krypton or hydrogen atoms; (iii) both MRK and GVF potential parameter sets were used for the carbon and oxygen atoms; (iv) only those rotational ($\Delta\chi$, deg) and translational displacements (ΔX, Å) compatible with the actual molecular site symmetry were allowed, thus preserving the overall space group symmetry.

The following flow chart summarizes how the data in Table 1 have been obtained:

Procedure
Calculation of packing potential energy (PPE) and of packing coefficient (pc) for the observed crystal structure
via OPEC[18]
Refinement of the observed crystal structure with crystal and site symmetry preserved
via PCK83[19]
Calculation of packing potential energy (PPE) and of packing coefficient (pc) for the observed crystal structure after refinement
via OPEC[18]

(14) Braga, D.; Grepioni, F.; Sabatino, P.; Gavezzotti, A. *J. Chem. Soc., Dalton Trans.* **1992**, 1185.

Table 1. Choice of Potential Parameters and Refinement of the Observed Crystal Structures

Ni(CO)$_4$

potent. type	M	OPEC[a] PPE[b]	PCK PPE[b]	ΔX (Å)	$\Delta\chi$ (deg)	OPEC PPE[b]	*a*-axis[c] (Å)
MRK	H	−14.4	−17.4	0.10	1.7	−15.6	10.459
GVF	H	−19.4	−20.5	0.05	1.0	−19.2	10.698
MRK	Kr	−22.4	−28.7	0.14	1.9	−25.1	10.269
GVF	Kr	−27.6	−30.9	0.09	1.4	−28.0	10.564

Fe(CO)$_5$

potent. type	M	OPEC[d] PPE[b]	PCK PPE[b]	ΔX (Å)	$\Delta\chi$ (deg)	OPEC PPE[b]	*a*-axis[c] (Å)	*b*-axis[c] (Å)	*c*-axis[c] (Å)	β (deg)[c]
MRK	H	−18.7	−22.7	0.15	1.5	−20.2	11.505	6.552	8.942	107.13
GVF	H	−24.3	−26.0	0.09	1.6	−24.6	11.883	6.720	9.197	107.37
MRK	Kr	−25.8	−33.9	0.19	1.6	−29.5	11.377	6.474	8.772	107.25
GVF	Kr	−31.9	−34.3	0.13	1.9	−33.0	11.816	6.645	9.041	107.53

[a] Refinement was based on the data set collected at 238 K (from ref 13). [b] In kcal·mol^{-1}. [c] After refinement with crystal symmetry preserved. [d] Refinement was based on the data set collected at 228 K (from ref 13).

Table 2. Energy[a] and Structural Features of the Dimolecular Nuclei (DMN)[a]

Ni(CO)$_4$ codes[b]	symmetry operator	Ni···Ni separation	ED (kcal·mol^{-1})	O···O separation	C···O separation	fig.[c]
Ni-OBS	I	4.62	−3.4	3.67−3.84	3.77−3.99	1a
Ni-T$_x$	T$_x$	5.05	−2.7	3.74−3.86	3.60−3.67	3b
Ni-T$_y$	T$_y$	6.00	−1.5	4.13−4.45	4.14−4.21	
Ni-T$_z$	T$_z$	6.98	−0.8	3.32−4.07	3.44−3.91	
Ni-I	I	4.52	−3.4	3.67−3.72	3.67−3.70	3a
Ni-S	S	4.60	−3.2	3.43−3.78	3.48−3.81	
Ni-2	2	5.01	−2.7	3.75−3.81	3.60−3.62	

[Ni(CO)$_4$]$_2$	symmetry operator	Ni···Ni separation	ED kcal·mol^{-1}	O···O separation	C···O separation
NiT-I	I	4.51	−3.9	3.08−3.68	3.68−3.77
NiT-S	S	4.87	−3.1	3.04−3.46	3.49−3.60

Fe(CO)$_5$ codes[d]	symmetry operator	Fe···Fe separation	ED (kcal·mol^{-1})	O···O separation	C···O separation	fig.[c]
Fe-OBS	I	5.16	−3.6	3.15−3.47	3.28−3.44	2a
Fe-T$_x$	T$_x$	7.18	−1.3	3.36−3.47	3.70−3.76	
Fe-T$_y$	T$_y$	6.83	−1.3	3.50−3.50	3.34−3.34	4c
Fe-T$_z$	T$_z$	6.63	−1.6	3.26−3.88	3.75−3.99	
Fe-I	I	5.09	−3.7	3.13−3.13	3.54−3.54	4a
Fe-S	S	5.18	−3.3	3.14−3.48	3.28−3.29	4b

[Fe(CO)$_5$]$_{sq}$	symmetry operator	Fe···Fe separation	ED (kcal·mol^{-1})	O···O separation	O···C separation	fig.[c]
Fe$_{sq}$-Ia	I	5.15	−4.1	3.31−3.47	3.39−3.48	5a
Fe$_{sq}$-Ib	I	4.84	−4.1	3.60−3.75	3.22−3.50	5b
Fe$_{sq}$-Ic	I	4.92	−3.9	3.70	3.29−3.51	
Fe$_{sq}$-S	s	5.71	−2.7	3.46−3.98	3.19−3.86	

[a] Nickel or iron as H atom; distances in Å. [b] Ni-T$_x$, Ni-T$_y$, and Ni-T$_z$ identify the three translational DMN; Ni-I and Ni-S = **I**- and **S**-DMN, respectively; Ni-2 = DMN obtained with molecular interlocking along a 2-fold axis of the tetrahedron; NiT-I and NiT-S = **I**- and **S**-DMN generated from the [Ni(CO)$_4$]$_2$ unit. [c] Only most representative DMN are shown in the corresponding figures. [d] Fe-T$_x$, Fe-T$_y$, and Fe-T$_z$ identify the three translational DMN obtained in the three directions of space; Fe-I and Fe-S = **I**- and **S**-DMN, respectively; Fe$_{sq}$-Ia, -Ib, and -Ic = alternative minima from the centrosymmetric DMN generation; Fe$_{sq}$-S = **S**-DMN.

Such a procedure allows direct comparison of the packing potential energies (PPE) before and after crystal structure refinement. From the data collected in Table 1 it is immediately apparent that, although the various sets of parameters yield essentially similar results, the setting which produces the smallest translational (ΔX, Å) and rotational ($\Delta\chi$, deg) displacements of the experimentally determined structures is GVF with the metal atom contribution set to that of a hydrogen atom. This is in keeping with our previous observation that the use of potential parameters for the metal atoms corresponding to atoms heavier than hydrogen causes excessive "shrinkage" of the crystal structure, yielding more tightly packed crystals, though at the expense of rather high repulsions between the outer O atoms.[14] In the following discussion the description of the results will be confined to those obtained with the set of parameters named GVF in which the metal atoms are treated as hydrogen.

(c) Generation of Dimolecular Nuclei. The construction of dimolecular nuclei is the initial step of the crystal generation procedure used. Dimolecular nuclei (DMN) are obtained by using PROMET.[20] The most common symmetry operators (the translation **T**, the center of inversion **I**, and the screw-axis **S**) are applied in the space surrounding the reference molecule. The "best nuclei" (best DMN) are selected on the basis of the interaction energy between the two symmetry related molecules forming the DMN. The energy of the dimer (ED) is obtained by means of the same potential function described above. It should be stressed that the DMN construction is not only the first step in the process of "crystal" generation but also the point at which unsatisfactory nuclei, and therefore crystals, are sifted out.

In our PROMET calculations the starting molecular structures of Ni(CO)$_4$ and Fe(CO)$_5$ were assigned an idealized geometry. The following parameters were obtained as average values from the most recent accurate structural refinements:[13] Ni−C 1.838 Å, C−O 1.141 Å, Ni−C−O 180°; Fe−C 1.821 Å, C−O 1.153 Å, Fe−C−O 180°; C−Ni−C 109.5°, C−Fe−C 90° and 120° (input coordinates and cells are given in the supplementary material). Calculations have also been carried out on a hypothetical square-pyramidal structure of Fe(CO)$_5$ [Fe(CO)$_5$]$_{sq}$ with Fe−C−O 1.821°, 1.153 Å, and apex-to-base angles of 105.0°. The computer program SCHAKAL was used for the graphical representation of the results.[21]

Molecule−Molecule Interaction and Nucleus Formation Description of the Dimolecular Nuclei (DMN)

The DMN search is not only the first step of the crystal construction process but it is also useful for exploring the basic process of molecule−molecule recognition, viz. the way in which to molecules can approach each other, interlock, and interact. Table 2 lists the interaction energy, the distance between centers of mass (i.e. metal atom separation), and the minimum interatomic contacts between oxygen and carbon atoms for the DMN obtained by pure translation, inversion, and screw operators for Ni(CO)$_4$, Fe(CO)$_5$, and [Fe-

(15) Mirsky, K. *Computing in Crystallography, Proceedings of the International Summer School on Crystallographic Computing*; Delft University Press: Twente, The Netherlands, 1978; p 169.
(16) Cox, S. R.; Hsu, L. Y.; Williams, D. E. *Acta Crystallogr., Sect. A* **1981**, *A37*, 293.
(17) Gavezzotti, A.; Filippini, G. *Acta Crystallogr., Sect. B* **1993**, *B49*, 868.
(18) (a) Gavezzotti, A. OPEC, Organic Packing Potential Energy Calculations. University of Milano, Italy. See also Gavezzotti, A. *J. Am. Chem. Soc.* **1983**, *195*, 5220.

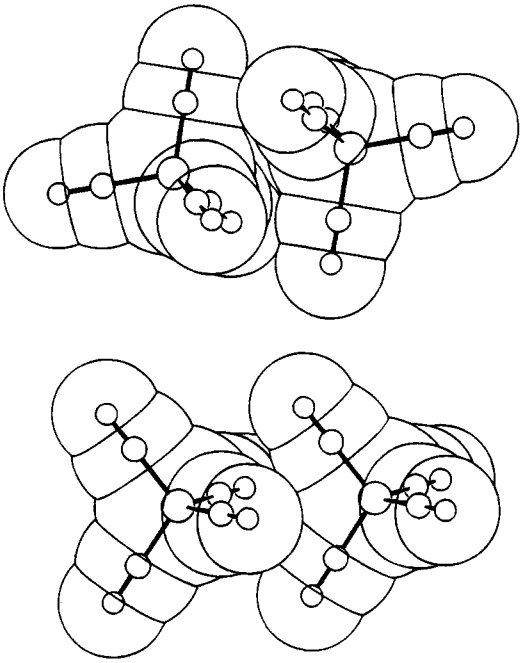

Figure 3. DMN of $Ni(CO)_4$. (a, top) Both **I** and **S** operators yield DMN (Ni-I, Ni-S) on the basis of the approach along the tetrahedron 3-fold axis. (b, bottom) The closest approach on two $Ni(CO)_4$ molecules via pure transition is achieved along the tetrahedron 2-fold axis (DMN Ni-T_x, Ni-2).

$(CO)_5]_{sq}$. These results are compared with the values observed for the closest neighbor pairs in the experimental crystal structures of the two complexes. Representative arrangements are shown in Figure 3 for $Ni(CO)_4$ and in Figure 4 for $Fe(CO)_5$. Similarly, DMN are examined for $[Fe(CO)_5]_{sq}$ and discussed in comparison with the trigonal-bipyramidal structure (see Figure 5).

In the case of $Ni(CO)_4$, both **I** and **S** operators yield similar DMN based on the approach along the tetrahedron 3-fold axis (see Figure 3a). This is exactly the fundamental "dimeric unit" observed in crystalline $Ni(CO)_4$ and shown in Figure 1a. It is remarkable that the search procedure has retraced so well the experimentally observed structure of the dimer. This is encouraging not only because it is a good indication that the potential parameters are reliable but also in view of the fact that the DMN generation is the preliminary (and fundamental) step of the crystal generation process. As shown in Table 2 the internuclear separation between the nickel atoms is also very close to that present in the observed structure.

Pure translation (see Figure 3b) does not yield DMN of comparable cohesion. The closest approach of two $Ni(CO)_4$ molecules via pure translation is achieved along the tetrahedron 2-fold axis. The minimum distance between two molecules interlocked along the 2-fold axis is 5.05 Å i.e. ca. 0.5 Å longer than that attained via **I** or **S** operators. This is reflected in an increase of the ED value from −3.4 and −3.2 to −2.7 kcal·mol^{-1}.

Obviously, it is possible to place a 2_1 axis on the origin of the unit cell through the nickel atom. The **S** operator, in such a case, has the same effect as a translation operator. Dimer Ni-2 is, in fact, essentially identical to dimer Ni-T_x (see Table 2).

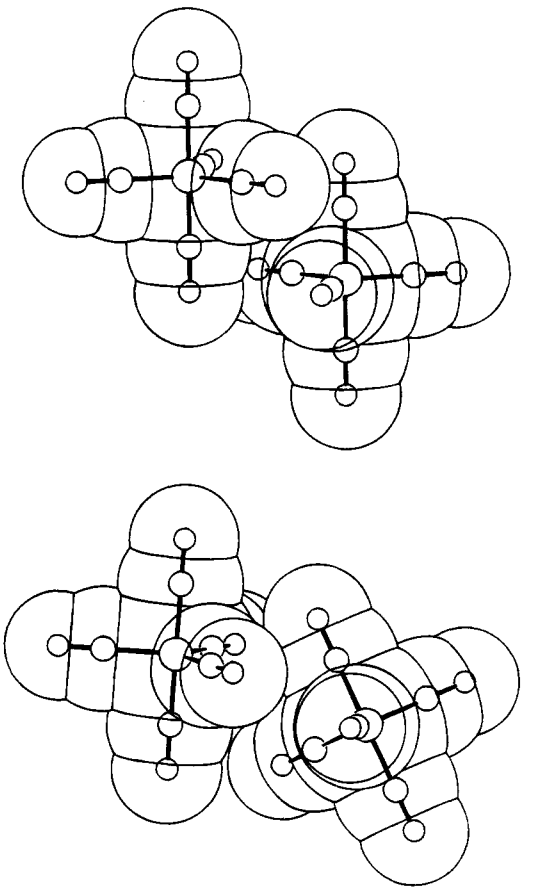

Figure 4. I, S, and **T** operators in the case of $Fe(CO)_5$. (a, top) The most cohesive I-DMN is based on the interlocking between one axial CO of one molecule and two equatorial ligands of a second molecule. Note that this DMN (Fe-I) is exactly that present in the experimental structure (compare with Figure 2a). (b, bottom) The **S**-DMN (Fe-S) is based on the interaction between two "trigonal" units formed by two equatorial and one axial CO.

The **I** and **S** operators yield different results in the case of $Fe(CO)_5$. The best **I**-DMN recalls the interlocking solution observed for $Ni(CO)_4$, viz. one axial CO of one molecule is "embraced" between two equatorial ligands of the second molecule (see Figure 4a), thus bringing the two Fe atoms at a distance of ca. 5.1 Å. Again this DMN is exactly that present in the experimental structure. We will see in the crystal generation section below that this also leads to reproduction of the observed crystal structure.

The **S**-DMN is constructed in a more complex way (see Figure 4b): the difference between **S**-DMN and **I**-DMN arises mainly from a small tilt of one molecule with respect to the other one, the interlocking still being based on the interaction between two "trigonal" units formed by two equatorial and one axial carbonyls.

Pure translation is (again) less efficient than **I** or **S** operators, yielding DMN which are definitely less stable (see Table 2). The least favorable interlocking is attained via direct insertion of one equatorial CO between

(19) Williams, D. E. PCK83, A Crystal Molecular Packing Analysis Program. Quantum Chemistry Program Exchange No. 481; Indiana University, Bloomington, IN.

(20) Gavezzotti, A. PROMET, A Program for the Generation of Possible Crystal Structures from the Molecular Structure of Organic Compounds; Mark version I, Milano. See also ref 9.

(21) Keller, E. SCHAKAL93, Graphical Representation of Molecular Models. University of Freiburg, FRG.

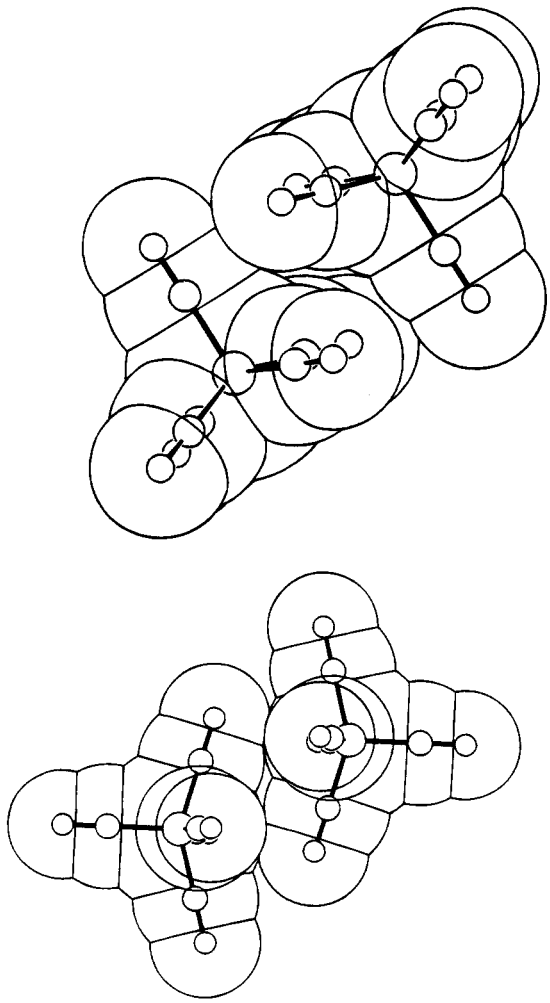

Figure 5. DMN of $[Fe(CO)_5]_{sq}$. (a, top) DMN Fe_{sq}-Ia: the inversion center relates two molecules aligned in antiparallel model. (b, bottom) DMN Fe_{sq}-Ib: the inversion center is placed underneath the square base. Note that in this DMN the two Fe atoms are at 4.86 Å.

two equatorial CO's of the neighboring molecule (see Figure 4c). Note that this translational relationship is present in the observed structure and, together with the DMN obtained via the **I** operator, combines to generate the C-centered monoclinic lattice illustrated in the previous section.

Contrary to those observed for $Ni(CO)_4$ and $Fe(CO)_5$, the potential energy hypersurface around $[Fe(CO)_5]_{sq}$ appears to be smoother and contains less well defined minima in the **I** search. Dimers Fe_{sq}-Ia, Fe_{sq}-Ib, and Fe_{sq}-Ic (see Table 2) represent three different, though not equally cohesive, ways of relating two molecules of $[Fe(CO)_5]_{sq}$ by means of an inversion center. The most stable DMN is shown in Figure 5a (structure Fe_{sq}-Ia). The inversion center relates two molecules aligned in antiparallel mode so that the unique axial ligand is "embraced" between two basal CO's of the neighbor. Alternatively, the inversion center can be placed underneath the square base, resulting in a DMN formed by two—almost "base-to-base"—square pyramids (structure Fe_{sq}-Ib; see Figure 5b). Interestingly, in this DMN the two Fe atoms are closer together not only than in Fe_{sq}-Ia (4.84 vs 5.15 Å) but also than in the observed structure (5.16 Å). The third minimum differs from the second one by a further sliding of the pyramid base that brings the O terminus of one molecule in direct van der Waals contact with the Fe atom of the second molecule. While the DMN named Fe_{sq}-Ia and Fe_{sq}-Ib have identical ED values (-4.1 kcal·mol^{-1}), this latter DMN is slightly less cohesive (-3.9 kcal·mol^{-1}). Note also that Fe_{sq}-DMN are, in general, more cohesive than those obtained with the trigonal-bipyramidal structure (see Table 2).

Table 3. Space Groups Resulting from Combination of T, I, and S Operators

space groups	symmetry operator	initial DMN
$P1$	T	T
$P\bar{1}$	I + T	I
$P2_1$	S + T	S
$P2_1/c$	S + I + T	S
$P2_1/c$	I + S + T	I
$P2_12_12_1$	S + S + T	S

The **S** search yields less cohesive DMN. In the DMN named Fe_{sq}-S (ED = -2.7 kcal·mol^{-1}) one basal dicarbonyl unit of one molecule embraces the Fe atom of the second one and fills in the space between the basal ligands. A further decrease in the energy of the dimer is observed when the DMN is constructed via pure translation.

Crystal Packing Search

All DMN discussed above were then translated in the three directions of space to generate *crystal* structures.

The space groups obtained by combining **I**- and **S**-DMN with the **T**, **I**, and **S** operators are shown in Table 3.

The space groups listed in Table 3 have been demonstrated (with the exception of $P1$) to be by far the most common space groups for organic molecules not forming hydrogen bonds.[23] These are also the space groups most often encountered in crystals of neutral organometallic molecules. Table 4 shows the results of a statistical survey of space group frequencies among 19 009 crystals structures formed by neutral mononuclear organometallic complexes. The results of the survey are compared with those available in the literature from analogous surveys of organic and mixed organic–organometallic crystal structures. It is clear that the distribution of crystal structures over the most frequent space groups is essentially the same in organic and organometallic crystals. The higher population of chiral molecules and natural products in the former crystals is reflected in a higher frequency of the noncentrosymmetric $P2_1$ and

(22) PROMET requires the presence of one molecular species (which might be two molecules as in part of this work) per crystallographic asymmetric unit and does not allow explicit convolution of molecular and crystal symmetry. Given the high molecular symmetry of the molecules studied here, crystal/molecular convolution may lead to the optimized trial structure which is a supergroup of those given in Table 3. Structures with symmetry higher than explicitly mentioned (in Tables 5–7) can and do result from the searching procedure provided that they produce low-energy DMN. This is well illustrated by the search for $Fe(CO)_5$ in $P\bar{1}$ which produces an optimum structure that has $C2/c$ symmetry. It seems unlikely that the supergroups of those in Table 3 will produce more cohesive packings than those found, given that the searching procedure allows orientational freedom for the molecular species within the crystallographic asymmetric unit. See ref 4a for a discussion of the effect of molecular symmetry preservation on the packing efficiency.

(23) (a) Kitaigorodsky, A. I. *Organic Chemistry Crystallography*; Consultant Bureau: New York, 1961. (b) Filippini, G.; Gavezzotti, A. *Acta Crystallogr., Sect. B* **1992**, *B48*, 230. (c) Scaringe, R. P. In *Electron Crystallography of Organic Molecules*; NATO ASI Series; Fryer, J. R., Dorset, D. L., Eds.; Kluwer Academic Publishers: Dordrech, The Netherlands, 1991; p 85. (d) Baur, W. H.; Kassner, D. *Acta Crystallogr., Sect. B* **1992**, *B48*, 356.

Table 4. Comparison of the Observed Space Group Frequencies in Organic and Organometallic Crystals

space group no.	space group symbol	organometallics (%)[a]	organics (%)[a]	organics (%)[c]	organics & organometallics (%)[d]
1	$P1$	0.6	*e*	1.5	1.2
2	$P\bar{1}$	19.7	15.0	13.4	16.9
	$P2_1$	2.9	8.7	10.0	6.4
14	$P2_1/c$	41.4	49.4	37.1	36.6
	$P2_1/a$				
	$P2_1/n$				
19	$P2_12_12_1$	6.0	7.8	18.1	11.0
61	*Pbca*	4.6	*e*	4.8	4.2
62	*Pnma*	2.4	*e*	1.1	1.6
33	$Pna2_1$	1.8	*e*	1.8	1.6
15	$C2/c$	7.8	*e*	5.6	7.0

[a] Search carried out on the 1993 version of the Cambridge Crystallographic Data System[26] on a sample of 19 009 crystal structures formed by neutral mononuclear organometallic molecules. [b] From 1068 non-hydrogen bonded crystals structures. The analysis is focused on the frequency of symmetry operators.[23b] [c] From a sample of 24 434 organic crystal structures.[23c] [d] From ref 23d. [e] Not examined in ref 23b.

$P2_12_12_1$ space groups. In general terms, however, the data compared in Table 4 confirm that neutral organometallic molecules obey essentially the same packing principles as organic molecules and pack in a similar way.[6]

Considering the data listed in Table 4, one may wonder about the opportunity of including in the search the less common space groups $P2_1$ and $P1$. Higher symmetry space groups may, however, result from the convolution of molecular symmetry and crystal symmetry.[22] It is also important to appreciate that we can only explore primitive cells with a maximum multiplicity of 4.[20] This limitation precludes the investigation of primitive space groups such as *Pbca* and *Pnma* with $Z = 8$, unless molecular and crystal symmetry are coincident.

Once the "theoretical" crystal structures have been obtained, they were compared with the experimental ones by the following calculation path:

PROMET	Potentials
Dimolecular Nucleus Search *via* **T**, **I**, and **S** operators	GVF, M as H
Calculation of the energy of the dimer, **ED**	
PROMET / PCK83	
3D-search	GVF, M as H
New primitive crystal structure, calculation of the cohesive energy, **CE**	
OPEC	
Calculation of **PPE**, comparison with observed structure	GVF, M as Kr

As discussed above, the packing search and generation was carried out by using the set of potential parameters designated as GVF. Since the metal atoms are treated as hydrogen atoms, the packing energies obtained in these calculations are meaningful only on a *relative basis*. For the sake of clarity we call "cohesive energy", CE, the packing energy calculated with this latter option for any given structure.

The results of the packing search for $Ni(CO)_4$, $Fe(CO)_5$, and $[Fe(CO)_5]_{sq}$ are collected in Tables 5–7 (the complete list of calculated crystal structures for all cases discussed herein is given as supplementary material). The structural solutions of minimum energy were selected on the basis of the values of CE and pc. With the exception of solution Fe-SB (see below), only structures within 3 kcal·mol^{-1} of the lowest energy structure have been listed in Tables 5–7. The volume of the asymmetric unit [V(asym) = V(cell)/Z] has also been used for a preliminary screening of the calculated crystal structures since the solutions for which V(asym) is much larger than that in the experimentally observed structures are associated with loosely packed and poorly cohesive crystals. The most representative solutions were examined graphically and are described below.

Alternative Crystal Structures for $Ni(CO)_4$

(i) $Ni(CO)_4$ Crystals: Triclinic $P1$. Although space group $P1$ is almost never observed, it is interesting to see that all hypothetical crystal structures attainable via the **T** operator are based on *head-to-tail* interlocking along the 2-fold axis of the $Ni(CO)_4$ tetrahedron. The shortest intermolecular separation along the axis is ca. 5.0 Å, i.e. identical to the value found in the DMN named Ni-2 (this is not surprising since the application of translational symmetry along a 2-fold axis has the same effect as a screw diad placed on the origin). The most cohesive $P1$ structure (Ni-TC, CE = −16.50 kcal·mol^{-1}, pc = 0.64) is shown in Figure 6. This crystal structure, however, is not competitive in terms of packing efficiency with Ni-OBS, nor are all the other calculated $P1$ structures (see supplementary material). The potential energy hypersurface is apparently fairly smooth with poorly defined minima, thus leading to many refined structures with similar cell dimensions and energies.

(ii) $Ni(CO)_4$ Crystals: Triclinic $P\bar{1}$. Much more significant are the structures obtained in space group $P1$ (i.e. **T** after **I**). The basic motif is the **I**-DMN discussed above, and all selected structures possess CE below −18 kcal·mol^{-1} and pc about 0.66 or higher (structures Ni-ID and Ni-IG in Table 5). Furthermore, when the high molecular symmetry is taken into account, higher symmetry C or F monoclinic or orthorhombic cells result. In structure Ni-IG V(asym) = 157.4 Å^3 is even smaller than in Ni-OBS (159.2 Å^3) and the highest pc (0.67) among the calculated structures results albeit less stable (CE = −15 kcal·mol^{-1}, cf. −19.4 for Ni-OBS). Figure 7 shows a projection of this structure Ni-IG down the pseudo-3-fold symmetry axis. This structure closely recalls Ni-OBS (Figure 1b). The primitive cell of structure Ni-IG can be transformed into an orthorhombic F-centered cell.

(iii) $Ni(CO)_4$ Crystals: Monoclinic $P2_1$. With the exception of solution Ni-SF, the packing search in space group $P2_1$ yields several packing arrangements which are similar in terms of cohesive energy and of efficiency of packing. Since identical DMN can be obtained by both **I** and **S** operators (see above), it is not surprising that some of these solutions are essentially identical to solutions obtained in $P\bar{1}$. The primitive cell of structure Ni-SC can be transformed into an orthorhombic C-centered cell with a V(asym) = 161.4 Å^3 and pc = 0.65,

Table 5. Summary of Crystal Data for Calculated Crystal Structures[a]

Ni-OBS[13]	PPE	pc	a (Å)	vol (Å^3)
$Pa\bar{3}$	−19.4	0.66	10.897	1293.96

calcd structure[b]/ alternative setting[c]	CE/lattice	pc	a/a′ (Å)	b/b′ (Å)	c/c′ (Å)	α/α′ (deg)	β/β′ (deg)	γ/γ′ (deg)	vol/vol′ (Å^3)
Ni-TC/triclinic	−16.50/P	0.64	5.029/5.943	5.943/6.471	6.471/5.029	111.89/110.32	110.32/91.32	91.32/11.89	165.68/165.68
Ni-ID/monoclinic	−18.41/C	0.66	7.395/13.25	6.597/6.587	7.831/7.831	89.48/90.00	71.54/110.43	63.59/90.00	320.62/641.27
Ni-IG/orthorh	−18.02/F	0.67	7.220/10.351	7.863/13.912	7.278/10.151	62.12/90.00	88.88/90.00	116.01/90.00	314.84/1461.82
Ni-SC/orthorh	−18.21/C	0.65	6.458/8.419	7.860/9.757	8.419/7.860	90.00/90.00	49.05/90.00	90.00/90.00	322.79/645.65
Ni-SF/orthorh	−18.07/C	0.66	8.656/8.656	7.850/7.850	6.381/9.433	90.00/90.00	47.65/90.00	90.00/90.00	320.44/640.89
Ni-2B/tetragonal	−15.61/P	0.61	5.740/5.729	10.454/5.729	8.133/10.500	90.00/90.00	45.31/90.00	90.00/90.00	346.90/344.59
NiT-IF/triclinic	−18.44/P	0.66	7.436/8.901	10.034/10.034	10.397/7.436	100.19/91.24	122.98/101.51	91.24/77.01	633.91/633.91
NiT-SA/triclinic	−17.90/P	0.65	6.530/6.530	7.849/7.849	13.045/12.891	90.00/90.00	74.11/103.27	90.00/90.00	643.06/643.06
Ni-S-I/orthorh	−17.87/C	0.66	6.481/6.481	14.441/13.604	7.488/14.441	90.00/90.00	114.73/90.00	90.00/90.00	636.53/1273.25

[a] Only the best solutions (pc > 0.60) are reported. Refer to supplementary material for a full list of calculated crystal structures. [b] Codes as follows: Ni-OPERATOR/SOLUTION (i.e. Ni-TC = crystal structure C obtained via pure translation T); Ni-T, triclinic $P1$, Ni-I triclinic $P\bar{1}$, Ni-S monoclinic $P2_1$, Ni-2 monoclinic $P2$, NiT-I, and NiT-S, idem on tetramolecular nuclei; Ni-S-I is monoclinic $P2_1/c$ obtained by coupling **S** and **I** operators. [c] Niggli reduced cell and alternative unit cell settings; differences in cell volumes are due to numerical approximations.

Table 6. Summary of Crystal Data for Calculated Crystal Structures[a] of $Fe(CO)_5$

Fe-OBS[13]	PPE	pc	a (Å)	b (Å)	c (Å)	α (deg)	β (deg)	γ (deg)	vol (Å^3)
$C2/c$	−24.3	0.67	11.785	6.828	9.388	90.	107.62	90.	719.99

calcd struct[b]/ alternative setting[c]	CE/lattice	pc	a/a′ (Å)	b/b′ (Å)	c/c′ (Å)	α/α′ (deg)	β/β′ (deg)	γ/γ′ (deg)	vol/vol′ (Å^3)
Fe-IA/monoclinic	−24.13/C	0.68	6.859/11.948	6.696/6.696	10.019/9.287	70.52/90.00	96.74/107.15	60.57/90.00	354.93/709.96
Fe-ID/monoclinic	−21.36/P	0.64	6.370/6.370	6.714/9.146	12.026/6.714	66.58/90.00	68.30/107.56	107.56/90.00	372.88/372.92
Fe-SB/orthorh	−18.28/C	0.60	7.645/6.710	8.687/13.884	7.767/8.690	90.00/90.00	51.58/90.00	90.00/90.00	404.14/809.55

[a] See footnote *a* to Table 5. [b] Codes as follows: Fe-OPERATOR/SOLUTION (see footnote *b* to Table 5), i.e. Fe-I, triclinic $P\bar{1}$, Fe-S monoclinic $P2_1$. [c] See footnote *c* to Table 5.

Table 7. Summary of Crystal Data for Calculated Crystal Structures of $[Fe(CO)_5]_{sq}$[a]

calcd structure[b]/ alternative setting[c]	CE/lattice	pc	a/a′ (Å)	b/b′ (Å)	c/c′ (Å)	α/α′ (deg)	β/β′ (deg)	γ/γ′ (deg)	vol/vol′ (Å^3)
Fe_{sq}-TC/triclinic	−21.19/P	0.67	5.782/5.782	6.364/6.629	8.920/5.603	95.60/93.26	57.16/112.05	54.69/65.65	180.10/180.12
Fe_{sq}-IaA/triclinic	−24.08/P	0.68	7.148/6.907	6.893/9.010	10.575/6.890	89.84/110.58	121.06/117.57	58.90/82.18	355.52/355.61
Fe_{sq}-IbD/triclinic	−24.39/P	0.69	5.815/7.152	9.193/9.045	10.413/5.820	55.05/107.25	104.05/91.25	70.04/79.04	352.65/352.77
Fe_{sq}-SB/monoclinic	−22.49/P	0.66	6.337/6.340	5.860/5.860	10.773/10.108	90.00/90.00	66.70/101.87	90.00/90.00	367.40/367.50

[a] See footnote *a* to Table 5. [b] Codes as follows: Fe-OPERATOR/SOLUTION (see footnote *b* to Table 5), i.e. Fe-I, triclinic $P\bar{1}$, Fe-S monoclinic $P2_1$. [c] See footnote *c* to Table 5.

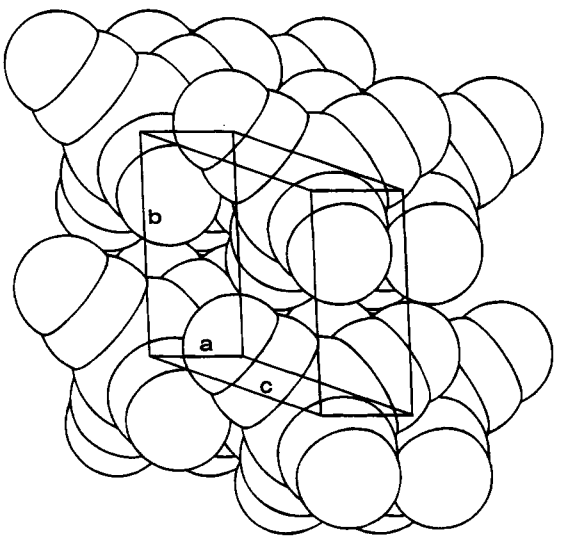

Figure 6. $Ni(CO)_4$ calculated crystal structure: the most cohesive $P1$ structure, Ni-TC.

i.e. similar to the value for Ni-OBS. Figure 8a shows how the packing arrangement in solution Ni-SC is built around a **S**-DMN which is very similar to the **I**-DMN examined above. Structure Ni-SF, on the other hand, can be transformed into an orthorhombic structure of relatively high cohesion (CE = −18.07 kcal·mol^{-1}). This solution differs from solution Ni-SC. A projection of solution Ni-SF is shown in Figure 8b. Although a highly symmetric molecule such as $Ni(CO)_4$ is unlikely to crystallize in space group $P2_1$, it should be kept in mind that the convolution of $P2_1$ with molecular symmetry may lead to much higher symmetry.[22] Examples are known of tetrahedral molecules that crystallize in relatively low symmetry space groups which are simple supergroups of $P2_1$; this is the case, for instance, of CBr_4[24a] and $SnBr_4$[24b] which crystallize in space groups $C2/c$ and $P2_1/c$, respectively.

(iv) $Ni(CO)_4$ Crystals: Translation along a 2-fold Axis of the Tetrahedron. The molecular interlocking observed in **T**-DMN can also be obtained when the **S** operator is applied on the origin of the cell through the nickel atom, yielding crystal structures that can be described in space group $P2$. Although this space group is not very common, it is interesting to observe that the action of the **S** operator passing through the center of the molecule is the same as that of a translational vector along a 2-fold axis of the tetrahedron. Consequently, the packing motif in cell Ni-2B is similar to that of Ni-T

(24) (a) More, M.; Baert, F.; Lefevre, J. *Acta Crystallogr., Sect. B* **1977**, *B33*, 3681. (b) Brand, P.; Sackmann, H. *Acta Crystallogr.* **1963**, *16*, 446.

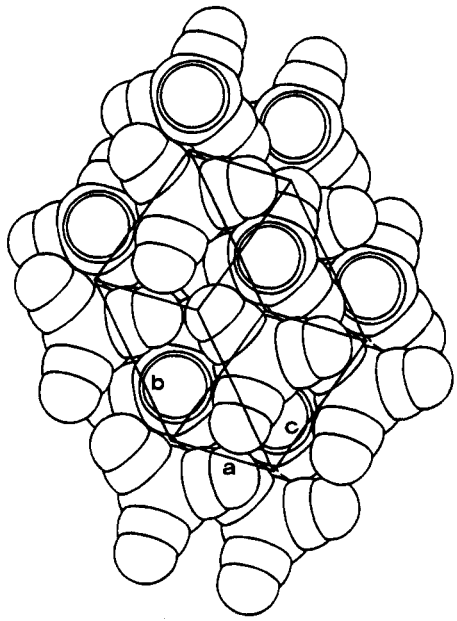

Figure 7. $Ni(CO)_4$ calculated triclinic crystal structure: a projection of structure Ni-IG down the pseudo-3-fold symmetry axis. Note how this structure is similar to that of Ni-OBS (compare with Figure 1b).

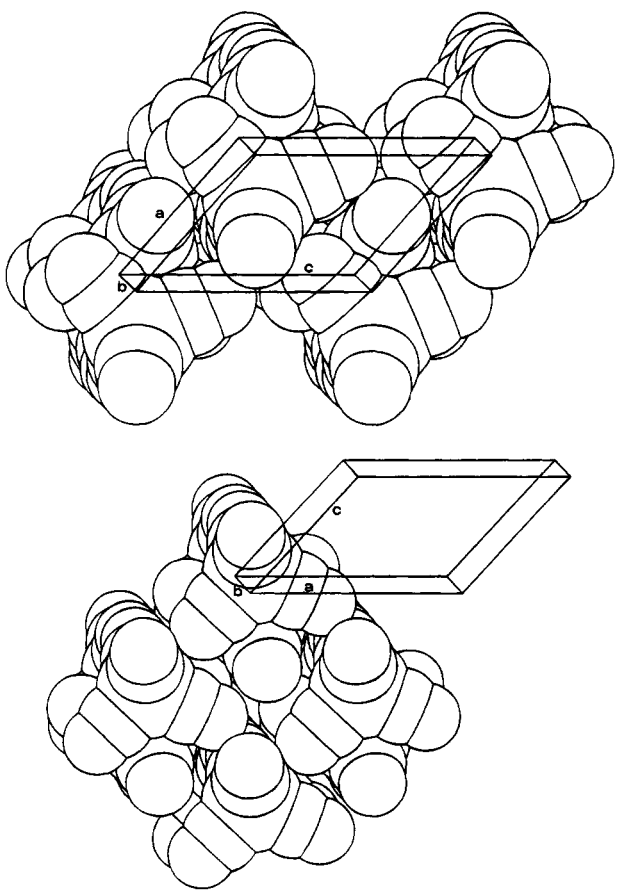

Figure 8. $Ni(CO)_4$ calculated crystal structure in space group $P2_1$: (a, top) packing arrangement in solution Ni-SC; (b, bottom) projection of solution Ni-SF.

cells. The unique *b*-axis in Ni-2B (10.454 Å) corresponds, in fact, to twice the intermolecular separation of ca. 5.0 Å (see Figure 9). Cell transformation on structure Ni-2B yields a tetragonal primitive cell with $Z = 2$. This structure is poorly cohesive (CE = −15.61 kcal·mol^{-1}, pc = 0.61), as observed for those obtained via translational search.

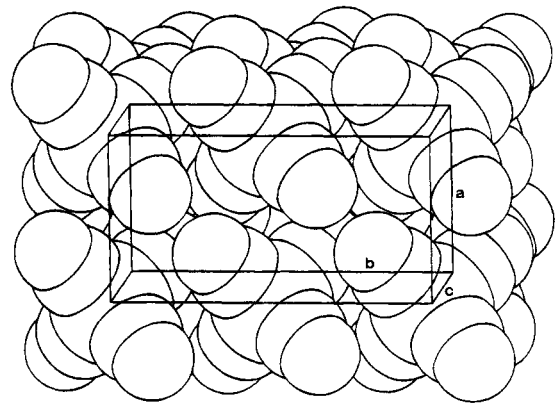

Figure 9. $Ni(CO)_4$ calculated crystal structure. The packing motif in solution Ni-2B is obtained by pure translation along a 2-fold axis of the $Ni(CO)_4$ tetrahedron.

(v) $Ni(CO)_4$ Crystals: Tetramolecular Nuclei (TMN). The observed structure of crystalline $Ni(CO)_4$ (Ni-OBS) is constructed around a dimeric unit in which the two constituent molecules are related by an inversion center. As we have shown before, this dimeric unit is strongly favored energetically and, very likely, represents the most effective way to interlock tetrahedral $Ni(CO)_4$ molecules. We have therefore attempted crystal generation via **I**, **T**, and **S** operators starting from such a *preformed* unit. Note that the following example illustrates the possibility of constructing, step-by-step, multimolecular nuclei by a different combination of symmetry operators.

The starting dimer is the Ni-ID illustrated above. In this dimer the intermolecular separation between the two constituent molecules is 4.61 Å. Analogously to the DMN, tetramolecular nuclei (TMN) can be generated via PROMET. The most cohesive TMN are named NiT-I and NiT-S. The Ni···Ni separation between Ni atoms belonging to next-neighbor DMN is 4.51 Å, i.e. only slightly shorter than within the starting DMN (4.61 Å). In the most cohesive **S**-TMN, on the contary, the Ni···Ni approach results longer than in Ni-SD (4.87 vs 4.60 Å).

Crystal generation based on these two TMN yields several structures. The most cohesive soltuion is represented by structure NiT-IF (CE = −18.44 kcal·mol^{-1}, pc = 0.66) shown in Figure 10a which is obtained by a translation search on NiT-I. Since, for centrosymmetric molecules, the I operator is coincident with the **T** operator, the same result can be obtained via the center of inversion. Similarly, the **T** operator on NiT-S affords the structure NiT-SA (Figure 10b), which appears to retrace the monoclinic structure obtainable from the **I** search carried out on the individual molecule (compare NiT-SA with Ni-ID).

(vi) $Ni(CO)_4$ Crystals: Monoclinic $P2_1/c$. As shown in Table 3 the **S** and **I** operators can be applied in sequence to generate crystal structures in the monoclinic space group $P2_1/c$. As pointed above, space group $P2_1/c$, together with triclinic $P\bar{1}$ and orthorhombic $P2_12_12_1$, is one of the most common in organic and organometallic crystallography (see Table 4).

The result of crystal structure generation in $P2_1/c$ for $Ni(CO)_4$ is reported in Table 5. Crystal structure Ni-S-I is obtained by performing the **I** search starting from

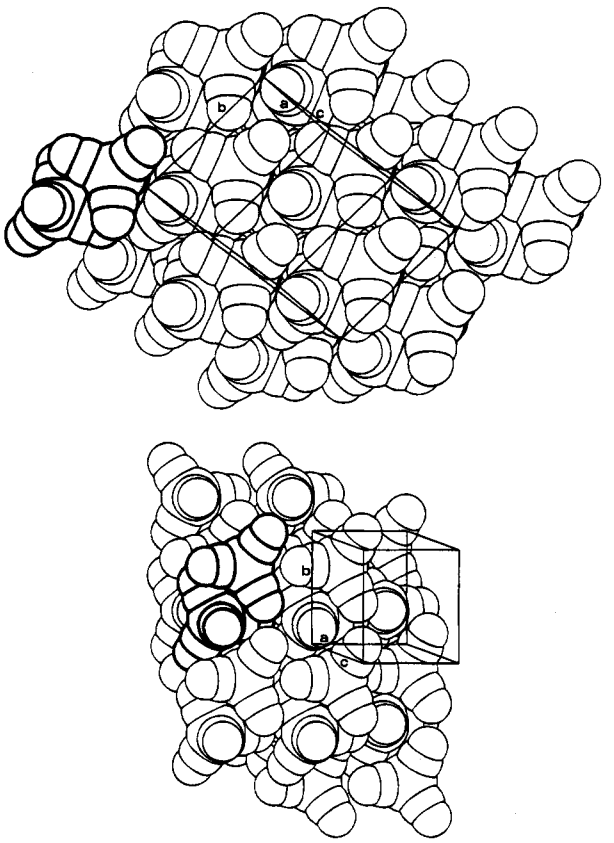

Figure 10. $Ni(CO)_4$ calculated crystal structure from tetramolecular nuclei. (a, top) The triclinic structure NiT-IF is obtained by a translational search on NiT-I. (b, bottom) The monoclinic structure NiT-SA retraces the monoclinic structure obtainable from the **I** search (thickened atom spheres mark the centrosymmetric unit used in the search procedure).

the same **S**-DMN as that generating structures Ni-SC and Ni-SF. Ni-S-I appears to be competitive in terms of CE and efficiency of packing with the other calculated structures reported in Table 5. After cell optimization the shortest intermolecular separation is between molecules related by the inversion center (4.44 Å), whereas the separation between the molecules related by the screw axis, as in the starting DMN, is larger (4.94 Å). Interestingly, Niggli reduction of solution Ni-S-I gives a C-centered orthorhombic cell of double volume (see Table 5).

(vii) $Ni(CO)_4$ Crystals: Orthorhombic $P2_12_12_1$. PROMET[20] allows us to apply a second **S** operator (along the *z*-direction) after the first one has been placed (perpendicular to the *xz* plane) and the first **S**-DMN generated. Since the first two screw-axes at 90° automatically define a third orthogonal axis, the orthorhombic space group $P2_12_12_1$ is generated. Although $P2_12_12_1$ is very often encountered in organometallic crystallography of chiral molecules, in the case of $Ni(CO)_4$ this arrangement does not yield any structure of particular interest. The calculated $P2_12_12_1$ structures were obtained by starting from the same S-DMN which yielded structures Ni-SC and Ni-SF in space group $P2_1$. All solutions are poorly cohesive and have pc values <0.40.

Alternative Crystal Structures for $Fe(CO)_5$

The results of the crystal structure search for $Fe(CO)_5$ are shown in Table 6 and will now be described. As in the case of $Ni(CO)_4$ crystal structures have been generated in space groups $P1$, $P\bar{1}$, $P2_1$, $P2_1/c$, and $P2_12_12_1$.

(i) $Fe(CO)_5$ Crystals: Triclinic $P1$ and Triclinic $P\bar{1}$. As in the case of $Ni(CO)_4$, the pure translational search (**T** operator) does not yield efficiently packed calculated structures in the space group $P1$. In no cases are pc values above 0.54 obtained.

Far more interesting is the result of the structure search in $P\bar{1}$. The "best" structural solution in this space group (Fe-IA) produces the Fe-OBS structure of $Fe(CO)_5$ in its reduced primitive cell. Cell transformation leads directly to the C-centered monoclinic structure present in Fe-OBS (see Table 6). This can be taken as a further proof that the structure search procedure (and the choice of potential parameters) is well suited for the structure simulation of simple binary carbonyls. It should be emphasized that this result has been obtained without space group restrictions in the search, i.e. by allowing only triclinic primitive cells. Although this is a significant achievement, it is not particularly surprising. Kitaigorodsky showed long ago that the space group $C2/c$ provides the best packing for molecules that exhibit 2-fold rotational symmetry.[4a] The calculated structure Fe-IA, shown in Figures 11a, is essentially identical to that of Fe-OBS geometrically as well as in terms of CE and pc (-24.13 kcal·mol^{-1} and 0.68 vs -24.3 kcal·mol^{-1} and 0.68; see Table 6). The projection shown in Figure 11b clearly shows that the two structures are essentially identical (compare with Figure 2b).

An alternative way to organize the fundamental centrosymmetric DMN of $Fe(CO)_5$ is shown in Figure 12. The triclinic cell of structure Fe-ID (see Table 6) can be transformed into a monoclinic primitive cell having $Z = 2$. Apart for Fe-IA all other solutions in space group $P\bar{1}$ are less cohesive and less efficiently packed.

(ii) $Fe(CO)_5$ Crystals: Monoclinic $P2_1$. As in the case of the pure translational search, the crystal structures of trigonal-bipyramidal $Fe(CO)_5$ obtained in space group $P2_1$ via the **S** operator appear to be less efficiently packed than those obtained via the center of inversion. This behavior contrasts with that observed above for the tetrahedral $Ni(CO)_4$. Figure 13 shows structure Fe-SB which is the most cohesive crystal generated by the search and cell optimization procedure in space group $P2_1$ (see Table 6). The molecules of $Fe(CO)_5$ are, however, ca. 10% less efficiently packed (pc = 0.60 and CE = -18.28 kcal·mol^{-1}) than in the structures obtained via **I** operator.

(iii) $Fe(CO)_5$ Crystals: Monoclinic $P2_1/c$ and Orthorhombic $P2_12_12_1$. As discussed above for $Ni(CO)_4$, symmetry operators can be combined to generate molecular arrangements in higher symmetry space groups (see Table 3). Starting from the Fe—S dimer, new crystal structures can be generated in monoclinic $P2_1/c$ and orthorhombic $P2_12_12_1$ by applying an **I** and **S** operator, respectively. Although the calculated structures are not competitive with the other structures reported in Table 6, it is still worth mentioning that searches in $P2_1/c$ and in $P2_12_12_1$ yield solutions with pc = 0.56 and 0.58, respectively.

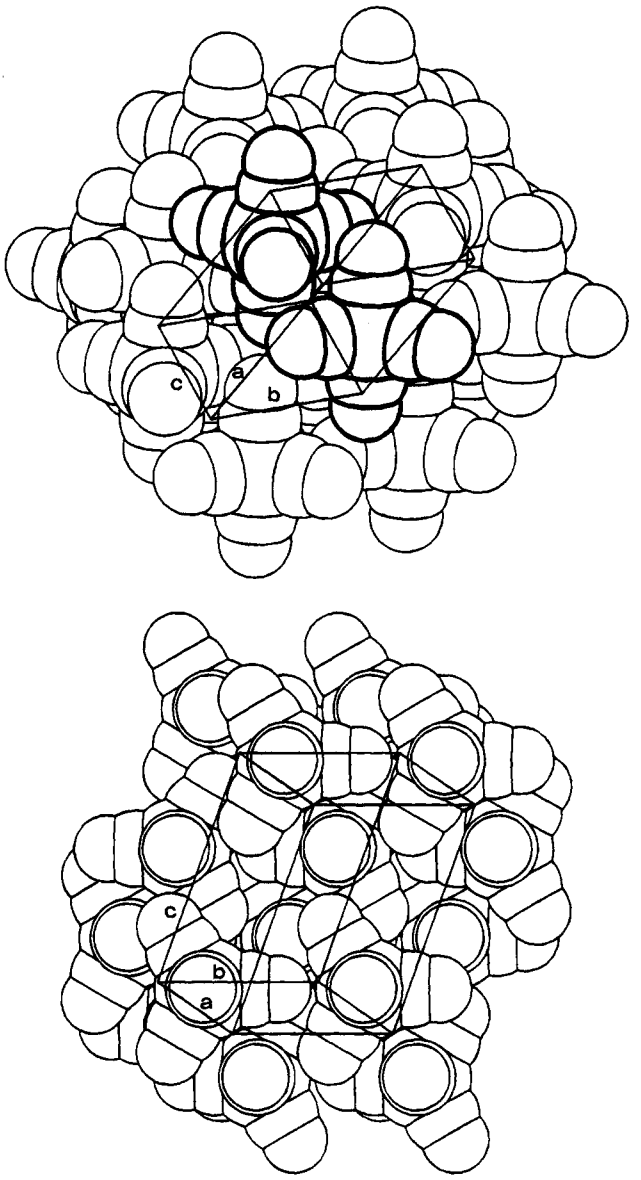

Figure 11. $Fe(CO)_5$ calculated crystal structure. (a, top) Structure Fe-IA retraces the observed crystal structure (compare the thickened molecular pair with Fe-OBS in Figure 2a). Compare the projection of structure Fe-IA in (b, bottom) with Figure 2b.

Alternative Crystal Structures Based on $[Fe(CO)_5]_{sq}$

It has been shown that when a molecule is flexible, crystal packing forces and the optimization of intermolecular interlocking in terms of shape and size can compensate for partial loss of "internal energy" and stabilize less stable molecular structures.[25] This may well be the case of $Fe(CO)_5$. In this section the results of crystal lattice generation starting from the *hypothetical* square-pyramidal molecular structure of $Fe(CO)_5$ $[Fe(CO)_5]_{sq}$ will be described. The aim of this experiment is essentially to verify whether it is possible to pack the Berry pseudorotation intermediate (namely the square pyramidal structure) efficiently and whether the calculated crystal structures are comparable in terms of packing cohesion with those discussed above for the trigonal bipyramid. One might expect, for example, that hypothetical crystals of the square pyramid may differ in stability from those of the trigonal bypyramid, indicating a packing preference for the crystallization of one of the isomers. In order to test this hypothesis, DMN of $[Fe(CO)_5]_{sq}$ were calculated as in the cases of $Ni(CO)_4$ and $Fe(CO)_5$ described above. The results are briefly described below.

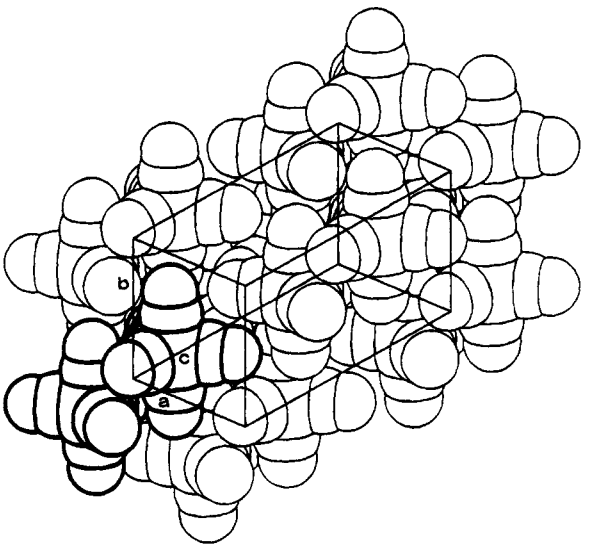

Figure 12. $Fe(CO)_5$ calculated crystal structure. Solution Fe-ID represents an alternative way to organize the fundamental centrosymmetric DMN of $Fe(CO)_5$.

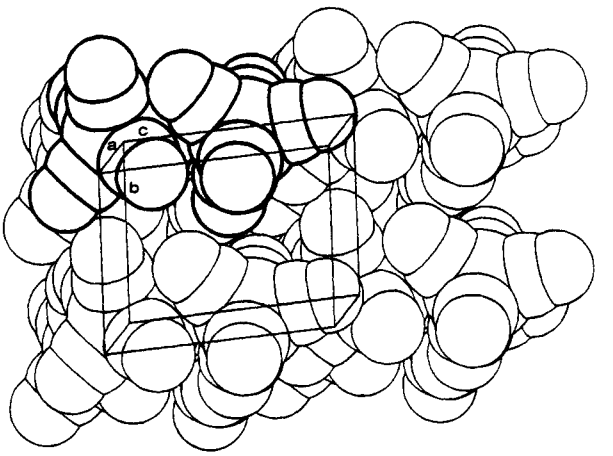

Figure 13. $Fe(CO)_5$ calculated crystal structure. Structure Fe-SB is generated by the search and cell optimization procedure in space group $P2_1$.

As discussed in the DMN section there are several minima in the **I** search map of $[Fe(CO)_5]_{sq}$. The most cohesive DMN are all based on the base-to-base interaction between two molecules and all yield fairly stable crystal packings. As shown in Table 7, structure Fe_{sq}-IA attains a high pc (0.68) and, correspondingly, a cohesive CE value (-24.08 kcal·mol^{-1}). Note that these two values are very close to those of Fe-OBS and to those found by the search procedure on the TBP molecule. The "best" triclinic crystal based on this DMN is shown in Figure 14a. This structure is based on the DMN named Fe_{sq}-IA with molecules in antiparallel orientation. It is interesting to observe here that in this

(25) Albano, V. G.; Braga, D. In *Accurate Molecular Structures*; Domenicano, A., Harghittai, I., Eds.; Oxford University Press: Oxford, U.K., 1992.

(26) Allen, F. H.; Bellard, S.; Brice, M. D.; Cartwright, C. A.; Doubleday, A.; Higgs, H.; Hummelink, T.; Hummelink-Peters, B. J.; Kennard, O.; Motherwell, W. D. S.; Rodgers, J. R.; Watson, D. G. *Acta Crystallogr., Sect. B* **1979**, *B35*, 2331.

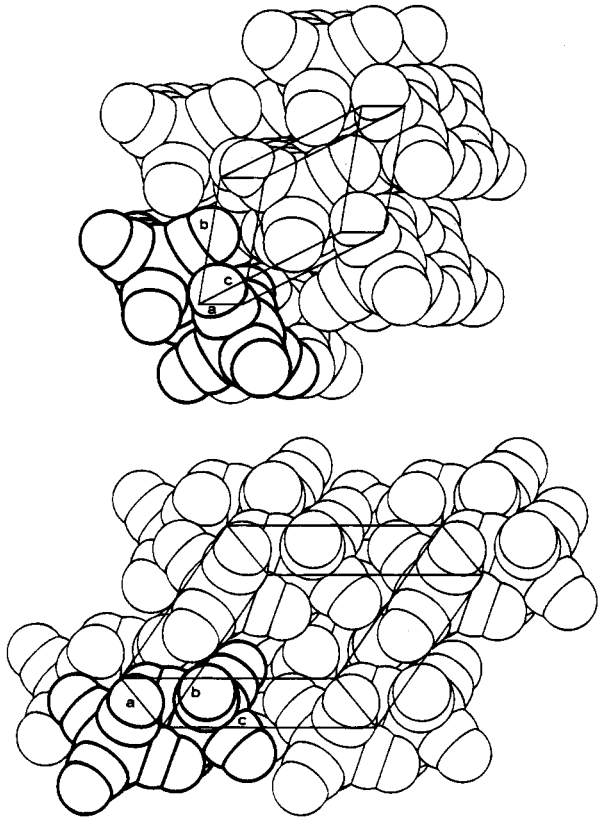

Figure 14. Crystal structure generation on $[Fe(CO)_5]_{sq}$. (a, top) Solution Fe_{sq}-IaA is based on the DMN named Fe_{sq}-IA with molecules in antiparallel orientation. (b, bottom) Solution Fe_{sq}-IbD is characterized by high packing efficiency and crystal cohesion.

structure (Fe_{sq}-IAA) the most cohesive interaction is not that derived from the original PROMET DMN (i.e. that depicted in Figure 5a, and highlighted in Figure 14a) but the dimer obtained via the operation $x - 1, y + 1, z - 1$ which has been generated only by the 3-D search and the subsequent cell relaxation and refinement. This demonstrates that the DMN generation procedure does not bias the subsequent 3-D search, since the final, most cohesive molecule—molecule interaction is not necessarily that between the components of the initial DMN. Pure translation is also fairly efficient in the packing of Fe_{sq} molecules, solution Fe_{sq}-TC, for example, has pc = 0.67 and CE = −21.19 kcal·mol^{-1} (see Table 7).

Other cohesive crystals can be obtained from dimer Fe_{sq}-IB. Solution Fe_{sq}-IBD, that is characterized by high packing efficiency and crystal cohesion (CE = −24.39 kcal·mol^{-1}, pc = 0.69), is shown in Figure 14b. In fact, solution Fe_{sq}-IBD not only represents the most cohesive crystal obtained from $[Fe(CO)_5]_{sq}$ molecules but also is even more densely packed than the *observed* monoclinic structure Fe-IA. Although the potential parameters used and therefore the energies obtained are to be treated with caution, this result demonstrates that nothing militates against the existence of an isomeric structure for $Fe(CO)_5$ at least as far as *intermolecular* interactions are concerned. Indeed, it is possible that these interactions may facilitate the interconversion TBP ↔ SQP of $Fe(CO)_5$ in the solid state by allowing stabilization of the intermediate.

Cohesive crystal structures can also be generated in space group $P2_1$ (see supplementary material). The most representative solution in Table 7 is solution Fe_{sq}-SB which possesses values of packing coefficient (0.66) and CE (−22.49 kcal·mol^{-1}) close to those obtained for the observed trigonal-bipyramidal structure.

Conclusions and Outlook

In this paper we have attempted the generation of crystal structures starting from the knowledge of the structure of individual molecules. The computational experiments were carried out on $Ni(CO)_4$ and $Fe(CO)_5$. These two molecules possess tetrahedral and trigonal-bipyramidal structures, respectively, i.e. two fundamental geometries for organometallic complexes; hence the results are (at least in principle) transferable to other systems of similar structure. We were interested in studying how molecules of this type can interact, interlock, and assemble in ordered three-dimensional arrays. The problem amounts to the investigation of the self-recognition and self-aggregation process behind the nucleation of a crystalline material and to the study of the intricate relationship between *the structure of one molecule and the structure of an ordered collection of such molecules*. Besides addressing these specific crystal chemistry problems, this research has also been directed to the setting of the simplest possible computational procedure that, beginning with the *decoding* of the observed crystal structure, could lead to the *generation* of alternative crystal structures of comparable cohesion and efficiency of packing. Crystal structure decoding is needed in order to identify the key packing motif (or motifs) responsible for intermolecular interlocking and crystal stability. Optimized dimolecular (DMN) and tetramolecular nuclei (TMN) have been generated, with the use of atom—atom potentials, to form the first nuclei around which theoretical crystal structures are subsequently built. Different choices of potential energy parameters have been tested to establish the most suitable for this purpose.

In the experimental crystal structure of both $Ni(CO)_4$ and $Fe(CO)_5$ the fundamental dimeric nucleus is generated by an inversion center. In keeping with this observation the most stable DMN generated at the nucleus search stage of our experiment are obtained via the inversion center. Those obtained via translation, 2-fold, and screw-axis are less stable. Interestingly, the screw operator "gains" on the inversion center when the molecular shape changes from tetrahedral in $Ni(CO)_4$ and trigonal bipyramidal in $Fe(CO)_5$ to octahedral as in $Cr(CO)_6$. The observed crystal structure of $Cr(CO)_6$ is, in fact, based on DMN generated by a 2_1-axis.[6] In the case of the hypothetical crystal formed by square-pyramidal molecules of $Fe(CO)_5$, on the other hand, the best DMN are again formed by centrosymmetric pairs.

The calculated DMN have been used in the subsequent three-dimensional search to generate new crystal structures. The results have been compared, in terms of cohesive energy and of efficiency of molecular packing, with those of the experimentally observed crystal structures. The main outcomes of the translational search can be summarized as follows.

(i) There are several alternative ways to construct three-dimensional (crystal) structures by efficient interlocking of tetrahedral or trigonal-bipyramidal molecules. Thus for both $Ni(CO)_4$ and $Fe(CO)_5$ molecules the existence of polymorphic modifications is a feasible possibility.

(ii) In the case of $Fe(CO)_5$ the crystal structure generation procedure successfully located the observed crystal structure on the basis of the centrosymmetric interlocking of molecules in a C-centered monoclinic system. This is particularly encouraging since the result has been obtained in a primitive triclinic lattice without symmetry constraints. As a matter of fact, the C-centered monoclinic structure is by far the best structural solution among the calculated crystal structures. Several other crystal structures generated have reasonable CE and pc values, but even the best of these (Fe-ID) has CE > 10% less cohesive than the observed structure.

(iii) The observed cubic structure of $Ni(CO)_4$ has not been directly located, although we have not attempted an exhaustive search of possible structures. It is clear that a number of solutions based on the centrosymmetric dimer reproduce the trigonal interlocking well and are close in CE and pc to the observed structure. This indicates that the potential functions employed in the search produce a potential energy hypersurface containing many minima of similar energy and do not discriminate clearly in favor of one. The parameter set might not be the most appropriate for a complex in which the metal atom is as exposed as it is in $Ni(CO)_4$. In this project we seek, however, *transferability* over more specific optimization of the potential parameters and therefore have not followed the latter course.

(iv) With the square-pyramidal structure of $Fe(CO)_5$ we have explored the possibility of predicting crystal structures for *hypothetical* molecules. Interestingly (and not without surprise), the crystal structure search has indicated that $[Fe(CO)_5]_{sq}$ can, in principle, be crystallized. The resulting crystals are essentially identical in terms of cohesion and packing efficiency with those of the observed crystal structure of the trigonal-bipyramidal molecule.

It is worth noting, on passing, that our analysis also suggests possible trajectories of approach for the reaction $2Fe(CO)_5 \rightarrow Fe_2(CO)_9 + CO$. It is easy to imagine that the formation of an **I**-DMN or of as **S**-DMN of the kind discussed above represents the preliminary stage (the "self-recognition" stage) of the dimerization reaction: visual inspection of the two nuclei (see Figures 4 and 5) suggests that formation of the Fe—Fe bond, CO elimination, and transformation of three ligands from terminal to bridging mode along the Fe—Fe bond can be achieved by simple activation of one of these DMN, perhaps with the intermediacy of a square-pyramidal structure.

In summary, we have shown that, given a molecule, it is possible to construct a number of crystal structures within a few kcal·mol^{-1} of the PPE associated with the observed structures, especially in the case of $Ni(CO)_4$. However, the fact that a relatively large number of possible alternative structures were obtained may indicate that the atom—atom potential function is not sufficiently discriminatory and can account satisfactorily only (or mainly) for the undirectional part of the intermolecular potential. More subtle effects (including entropy and directional interactions) need to be considered. Nonetheless, it is relevant that empirical computational approaches developed in the neighboring field of solid state organic chemistry can be transferred to organometallic systems with comparable results.[20] We envisage a number of applications for this and similar methods. If coupled with molecular structure optimization procedures (quantum chemistry, molecular mechanics, etc.), the method can in principle lead to an ab-initio suggestion of the crystal structure(s) of neutral organometallic molecules. Other applications might be the crystal structure determination of powdered materials and the study of phase transformations, polymorphism, and the relationship between the structure of ordered and disordered crystal phases. The most promising prospects for this type of study are, however, in the field of *supramolecular chemistry*, viz. the study of molecular recognition in organometallic and inorganic chemistry, including solid-state reactivity, surface chemistry, and the chemical consequences of the molecular shapes.

Acknowledgment. It is a pleasure to thank Prof. Angelo Gavezzotti for many useful discussions and for continuous help and encouragement; without his work with PROMET this study would not have been possible. We thank Eddie Dillon (Dublin) for his contribution to this paper within the ERASMUS exchange project "Crystallography". D.B. and F. G. acknowledge CNR for financial support, A.G.O. thanks the Ciba-Geigy Foundation for the award of a Senior Research Fellowship.

Supplementary Material Available: Tables of crystal data for all calculated crystal structures for $Ni(CO)_4$, $Fe(CO)_5$, and $[Fe(CO)_5]_{sq}$ and of parameters for the packing potentials (5 pages). Ordering information is given on any current masthead page.

OM940421N